



OPEN

Fission yeast Cdc14-like phosphatase Flp1/Clp1 modulates the transcriptional response to oxidative stress

Juan A. Canete^{1,2}, Sonia Andrés^{1,2}, Sofia Muñoz^{1,2}, Javier Zamarreño^{1,2}, Sergio Rodríguez^{1,2}, Helena Díaz-Cuervo^{1,2,3}, Avelino Bueno^{1,2}✉ & María P. Sacristán^{1,2}✉

Reactive oxygen species (ROS) are an important source of cellular damage. When ROS intracellular levels increase, oxidative stress takes place affecting DNA stability and metabolic functions. To prevent these effects, stress-activated protein kinases (SAPKs) delay cell cycle progression and induce a transcriptional response that activates antioxidant mechanisms ensuring cell adaptation and survival. Fission yeast Cdc14-like phosphatase Flp1 (also known as Clp1) has a well-established role in cell cycle regulation. Moreover, Flp1 contributes to checkpoint activation during replication stress. Here, we show that Flp1 has a role in fine-tuning the cellular oxidative stress response. Phosphorylation-dependent nucleolar release of Flp1 in response to oxidative stress conditions plays a role in the cellular transcriptional response. Thus, Flp1 ablation increases the transcriptional response to oxidative stress, in both intensity and duration, upregulating both Atf1/Pcr1- and Pap1-dependent stress induced genes. Remarkably, we found that Flp1 interacts with the Atf1/Pcr1 complex with Pcr1 acting as a direct substrate. Our results provide evidence that Flp1 modulates the oxidative stress response by limiting the Atf1/Pcr1-mediated transcription.

All aerobic organisms deal with reactive oxygen species (ROS)-mediated cell damage. ROS are natural byproducts of oxygen metabolism produced during respiration in aerobic organisms and are also triggered by external environmental factors. In eukaryotes, ROS induce the activation of stress-activated protein kinases (SAPKs), a subfamily of mitogen-activated protein kinases (MAPKs), that guarantee adaptation to stress and cell survival¹. In *Schizosaccharomyces pombe*, a unique SAPK pathway responds to different forms of stress, including osmotic, thermal and oxidative stresses. In this pathway, a central MAPK called Sty1/Spc1 (hereafter referred to as Sty1) is activated under stress conditions. Sty1 is able to induce the activation of several transcription factors that start the transcription programs of both global response genes, those that are expressed under general stress conditions, and specific response genes, those expressed only under certain stress conditions^{2–5}. Sty1 is activated by the phosphorylation of Thr-171 and Tyr-173 residues, which is carried out by MAPKK Wis1^{3,6,7}. In turn, Wis1 is activated by two MAPKKs, Wis4 and Win1^{8–10}. Among the effectors of Sty1 is Atf1, a basic Zipper (bZIP)-containing transcription factor, which is responsible for transcriptional responses to stress conditions. Direct phosphorylation of Atf1 by Sty1 is necessary to activate transcription^{11,12}. Atf1 is homologous to ATF-2, a substrate for the human SAPKs p38 and C-Jun N-terminal kinases, proving the conservation of the stress response kinases throughout evolution^{4,13,14}. Atf1 heterodimerizes with Pcr1, another bZIP transcription factor, and the resulting Atf1/Pcr1 complex is primarily involved in the induction of Sty1-dependent genes in oxidative stress conditions^{11,15,16}.

The amplitude and duration of SAPK-mediated transcriptional signaling are tightly regulated in the oxidative stress response¹⁷. The inactivation of Sty1 is triggered thanks to the contribution of two tyrosine phosphatases, Pyp1 and Pyp2, and two serine/threonine phosphatases, Ptc1 and Ptc3, that remove phosphates from the Tyr-173 and Thr-171 residues of Sty1, respectively^{2,3,7,18,19}. The attenuation of Sty1 signaling is mediated through the Sty1-Atf1 pathway, which constitutes a negative feedback system. Moreover, it has been shown that an additional phosphatase, Ptc4, deactivates the mitochondrial pool of activated Sty1²⁰.

¹Instituto de Biología Molecular y Celular del Cáncer (IBMCC), Universidad de Salamanca-CSIC, Campus Miguel de Unamuno, 37007 Salamanca, Spain. ²Departamento de Microbiología y Genética, Universidad de Salamanca, Campus Miguel de Unamuno, 37007 Salamanca, Spain. ³Present address: Axentiva Solutions SL, 08036 Barcelona, Spain. ✉email: abn@usal.es; msacristan@usal.es

In addition to Sty1 MAPK, the cellular response to oxidative stress also entails the action of Pap1, another bZIP transcription factor, homologue to mammalian c-Jun, that in response to oxidative stress accumulates into the nucleus to trigger a specific antioxidant gene response²¹. Both Sty1-Atf1 and Pap1 pathways regulate the expression of both distinct and overlapping sets of genes in response to different levels of oxidative stress^{11, 22, 23}. Moreover, Sty1-Atf1 could negatively regulate Pap1 target genes²².

Flp1/Clp1 phosphatase (hereafter referred to as Flp1), the ortholog of *S. cerevisiae* Cdc14, is a non-essential protein important for the proper regulation of mitotic exit and cytokinesis in *S. pombe*, by reversing specific Cdk1 substrate phosphorylation during anaphase^{24–27}. In normal cell cycle conditions, Flp1 is sequestered within the nucleolus and the spindle pole body (SPB) during interphase. Then, before anaphase, it is released from sequestration to access its substrates and carry out its functions^{24, 25}. Likewise, it has been shown that Flp1 undergoes dynamic subcellular localization changes in response to specific stress conditions. Thus, under replicative stress, Flp1 is released from the nucleolus into the nucleus to regulate the full activation of the checkpoint kinase Cds1²⁸. It has been also observed that interphase Flp1 is relocalized from the nucleolus to the nucleoplasm in response to oxidative stress, but not to osmotic or thermal stress²⁹. The redistribution of Flp1 under these two genotoxic stress conditions is controlled by specific and complex phosphoregulatory networks, in which different kinases such as Cds1, Chk1, Pmk1 and Cdk1 seem to be involved^{28, 29}. Although the role of nucleoplasmic Flp1 accumulation upon replicative stress conditions is already known²⁸, the function of nuclear Flp1 under oxidative stress is still to be discovered. In this work, we have explored the functional meaning of Flp1 subcellular relocalization from the nucleolus to the nucleus under oxidative conditions caused by H₂O₂ treatment and found that in cells lacking Flp1 phosphatase, the SAPK-mediated transcriptional induction of specific oxidative stress response genes is upregulated in both magnitude and duration. Significantly, Flp1 interacts *in vivo* with the Atf1/Pcr1 transcription complex and dephosphorylates Pcr1 *in vitro*. Our findings suggest that the cell cycle regulator Flp1 phosphatase contributes to the fine-tuning of the oxidative stress response in fission yeast by acting on the Atf1/Pcr1 transcriptional complex.

Results

Loss of *flp1* phosphatase partially rescues the sensitivity of SAPK mutants to oxidative stress and upregulates the stress-related transcriptional response.

First, it was confirmed that oxidative stress, caused by 1 mM H₂O₂ treatment, induced the release of Flp1-GFP from the nucleolus to the nucleoplasm and that this change of location depended on Flp1 phosphorylation²⁹ (Supplementary information Fig. S1a,b). A complex phosphoregulation of Flp1 governs this relocalization. It has been reported that Cds1 and/or Chk1 kinases preferentially act upon replicative stress conditions, whereas Pmk1 and Cdk1 phosphorylate Flp1 upon H₂O₂ treatment^{28, 29}. Importantly, however, mutation of all nine Cds1/Chk1-RxxS phosphosites in Flp1 (Flp1-9A-GFP mutant, Supplementary information Fig. S1c) was enough to prevent the nucleolar release of the Cdc14-like phosphatase in response to oxidative stress in 95% of cells (Supplementary information Fig. S1), as previously observed upon induction of replicative stress²⁸. This percentage of cells showing nucleolar Flp1 retention was higher than that observed in Flp1-6A-GFP, in which only six Flp1 RxxS phosphosites were mutated (Supplementary information Fig. S1). These data indicate that phosphorylation of Flp1 at RxxS phosphosites regulates its relocalization from the nucleolus to nucleoplasm also under oxidative stress conditions.

In response to oxidative stress, Sty1 is activated by Wis1 kinase to induce the activation of several transcription factors that will induce transcription programs of both global and specific oxidative stress response genes^{18, 19, 23, 30}. Moreover, Sty1 activates Srk1 kinase to prevent the transition from G2 to mitosis by direct inhibitory phosphorylation of Cdc25, a key mitotic activator^{31, 32}. To gain insight into the biological function of the nuclear Flp1 accumulation under oxidative stress conditions, we first performed a genetic interaction analysis on stress activated Wis1, Sty1, and Srk1 kinases. Deletion of either *wis1* or *sty1*, but not *srk1*, genes decreased tolerance to oxidative stress (Fig. 1a). Interestingly, the abrogation of *flp1* did not cause additional effects but rather a weak rescue of the sensitivity of *wis1* and *sty1* mutants to the chronic presence of H₂O₂ (Fig. 1a). Moreover, Pap1 absence completely suppressed the growth recovery of $\Delta flp1 \Delta sty1$ cells, while the lack of Pcr1 and Atf1 increased it (Supplementary information Fig. S2). These results confirm the crosstalk between the Wis1-Sty1-Atf1 and Pap1 signaling routes and suggest Flp1 may have a role in the negative modulation of the oxidative stress response likely through the Sty1-Atf1 pathway.

Many genes are involved in oxidative stress response, whose expression is directly stimulated by the Sty1-Atf1 pathway³⁰. Atf1 is a Zip-family transcription factor, activated by Sty1-mediated phosphorylation, essential to transcription initiation during stress^{11, 12}. The ability of Flp1 to partially rescue stress response defects in $\Delta sty1$ and $\Delta wis1$ mutants prompted us to test whether it could influence the induction of Sty1-Atf1-mediated oxidative stress genes, such as *ctt1*⁺, *gpd1*⁺, *hsp9*⁺, and *pyp2*⁺, coding for catalase, glycerol-3P-dehydrogenase, heat shock protein 9, and a tyrosin phosphatase, respectively. Consequently, we performed a comparative quantitative real-time PCR analysis (qPCR) to check the expression of these genes in both wild-type and $\Delta flp1$ cells under oxidative stress conditions caused by a 1 mM H₂O₂ treatment. As shown in Fig. 1b, and confirming previous observations³⁰, mRNA expression levels of all these genes increased in wild-type cells at early incubation times (15–30 min) and progressively recovered thereafter until pre-stress levels were reached. However, in cells lacking the *flp1*⁺ gene, the mRNA levels were not only higher after a 15-to-30-min treatment but were also sustained for a longer duration as compared to wild-type cells. In fact, in the absence of Flp1, the cells did not recover initial mRNA expression levels (0 min time point) during the entire treatment. Since the transcription levels of these genes did not increase in cells lacking *flp1* under normal conditions, compared with wild-type cells (Supplementary information Fig. S3a), we concluded that these differences between wild-type and $\Delta flp1$ cells were specific to an oxidative stress response.

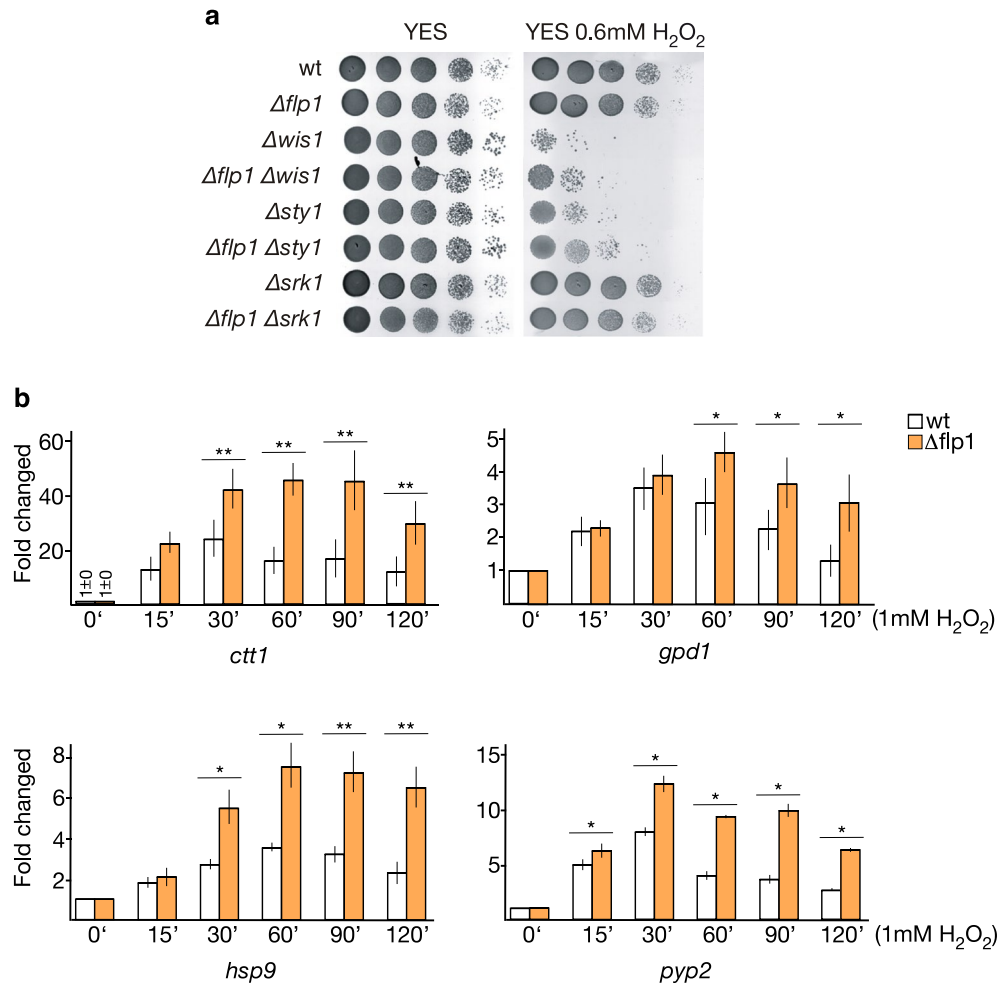


Figure 1. Loss of Flp1 phosphatase alters the cellular response to oxidative stress. (a) *flp1* deletion partially rescues sensitivity of $\Delta wis1$ and $\Delta sty1$ strains to chronic presence of H₂O₂. Tenfold serial dilution of indicated strains were spotted onto YES-agar plates without or with 0.6 mM H₂O₂ and incubated at 30 °C. (b) Altered transcriptional profiles in Flp1-deficient cells in response to oxidative stress. Total RNA of samples taken at indicated time points from wild-type and $\Delta flp1$ cells treated with 1 mM H₂O₂ was extracted and reverse transcribed using a mix of oligo(dT) and random hexamers primers. mRNA levels of *ctt1*⁺, *gpd1*⁺, *hsp9*⁺ and *pyp2*⁺ genes were measured by qPCR and normalized with ribosomal 18S mRNA. In both wild-type and Flp1-deficient cells, the amount of each mRNAs at time 0' (untreated conditions) was considered 1 and the rest of values were determined with respect to this value. Data were expressed as means SD in triplicate. Asterisks indicate statistical significance (*P < 0.05; **P < 0.005, *t*-test unpaired) versus wild-type.

It has been shown that under H₂O₂ treatment, Atf1 regulates the transcription of Sty1-dependent genes by forming a heterodimer with Pcr1, another basic-leucine ZIP transcription factor^{15, 16, 33}. Both *Atf1* and *Pcr1* transcripts are also induced in response to H₂O₂ treatment^{23, 30, 34}. Thus, we also analyzed the induction of these two transcripts upon oxidative stress conditions in both wild-type and cells lacking *flp1*. We found that the absence of *flp1* did not significantly affect the expected transcriptional upregulation of these two genes at early incubation times (15–30 min) but did affect their recovery kinetics, which were much more attenuated compared to wild-type cells (Fig. 2a), as previously observed for genes *ctt1*⁺, *gpd1*⁺, *hsp9*⁺ and *pyp2*⁺ (Fig. 1b). In the case of *atf1*⁺, these results were confirmed by Northern blot analysis (Fig. 2b,c). Expression analyses performed in the presence of phenanthroline, a potent transcriptional inhibitor³⁵, confirmed that the increase in *atf1* mRNA levels was not due to an increase in basal mRNA stability but to an increase in gene expression (Fig. 2c). Moreover, Flp1-mediated modulation of the transcriptional response to oxidative stress depended, as expected, on the activation of the Sty1 MAP kinase, as *atf1*⁺ transcription was comparably repressed in $\Delta sty1$ and $\Delta sty1 \Delta flp1$ mutant cells (Supplementary information Fig. S3b). These findings highlight that, in fission yeast, nucleoplasmic Flp1 can negatively control the Sty1-Atf1-dependent transcriptional response to oxidative stress conditions.

In addition to Atf1 and Pcr1, the bZIP Pap1 transcription factor is likewise connected to the oxidative stress response^{11, 21, 22}. To investigate whether Flp1 also regulates the Pap1-dependent expression genes such as *apt1*⁺ and *trr1*⁺ coding for an adenine phosphoribosyltransferase, and a thioredoxin reductase, respectively^{21, 36, 37}, comparative qPCR analyses were performed to examine the expression of these genes in both wild-type and $\Delta flp1$ cells under 1 mM H₂O₂ treatment. In the case of *apt1*⁺, we observed that the reported mRNA level reduction

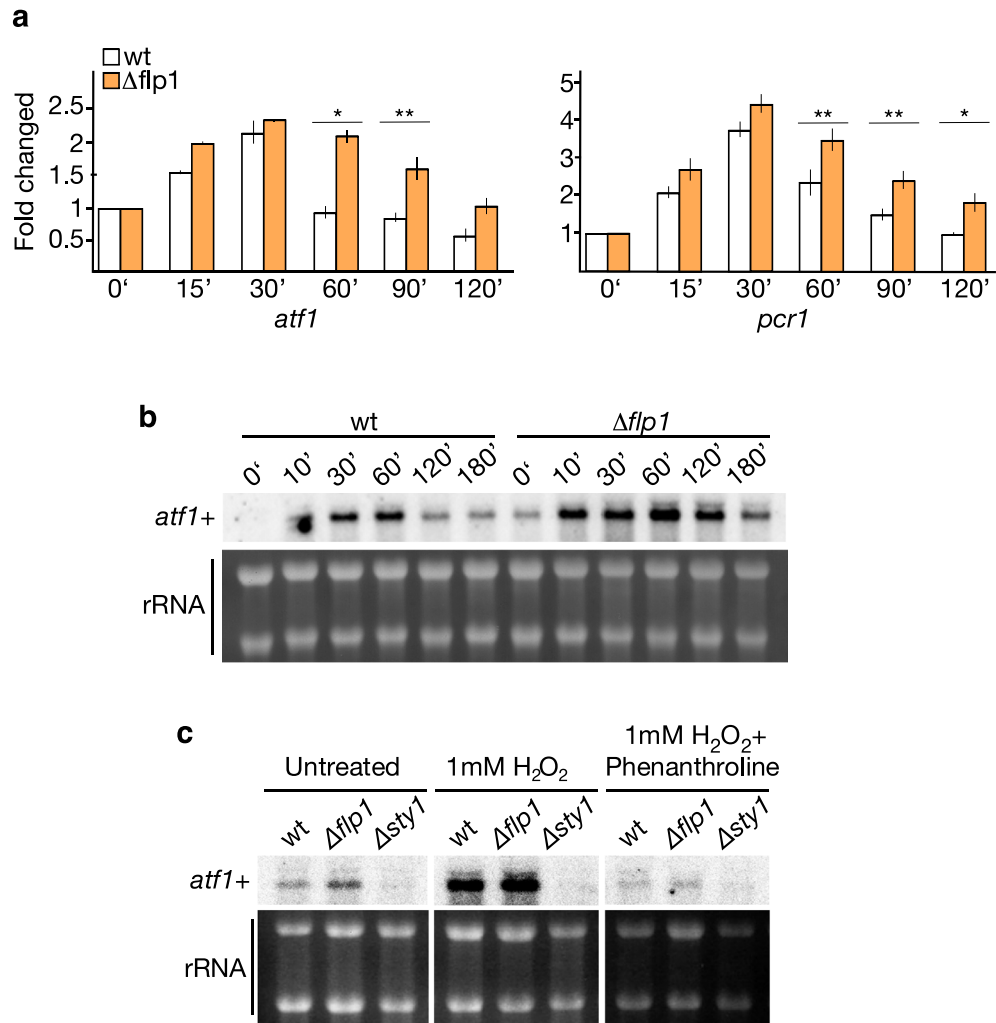


Figure 2. Depletion of Flp1 alters the transcriptional profile of *atf1*⁺ and *prc1*⁺ transcription factors in response to oxidative stress. **(a)** mRNA levels of *atf1*⁺ and *prc1*⁺ were measured by qPCR from total RNA extracted from wild-type and $\Delta flp1$ strains growing in YES medium containing 1 mM H₂O₂. Total RNAs were prepared from treated cells at the time points indicated. mRNA levels were normalized with ribosomal 18S mRNA and determined with respect to time 0' value, which was considered as 1. Data were expressed as means SD in triplicate. Asterisks indicated statistical significance (*P < 0.05; **P < 0.005, *t*-test unpaired) versus wild-type. **(b)** mRNA levels of *atf1*⁺ were measured by northern blot from total RNA extracted from wild-type and $\Delta flp1$ strains growing in YES medium containing 1 mM H₂O₂. Total RNAs were prepared at the time points indicated and processed for Northern blot analysis. Loading control are rRNAs stained with methylene blue. Full-length blots are shown in Supplementary Fig. S8. **(c)** Exponentially growing cultures of strains indicated were treated with either 1 mM H₂O₂ or 1 mM H₂O₂ / 1,10-phenanthroline (a potent transcription inhibitor). Total RNA was obtained, separated by electrophoresis and northern blots were assayed with a specific *atf1*⁺ probe. Expression of *atf1*⁺ transcription factor gene in $\Delta flp1$ is abolished when treated with 1,10-phenanthroline showing that it is regulated only at the transcriptional level. Loading control are rRNAs stained with methylene blue. Full-length blots are shown in Supplementary Fig. S8.

in response to oxidative stress³⁰ was significantly reduced in $\Delta flp1$ mutant cells, and even an increase of basal levels was found at the earliest incubation time (Fig. 3). For *trr1*⁺, whose levels increase in response to H₂O₂ treatment, the absence of *flp1* significantly accentuated its transcriptional upregulation compared to wild-type cells (Fig. 3). The same was observed when examining *srx1*⁺ mRNA encoding a sulfiredoxin reductase, which expression depends on both Atf1 and Pap1 transcription factors³⁸. These results strongly suggest that the lack of Flp1 phosphatase also affects the Pap1-dependent pathway in response to oxidative stress conditions. Since Sty1-Atf1 and Pap1 come into two cross-talking oxidative stress activated pathways, between which Atf1 could negatively regulate Pap1 activity²², the role of Flp1 on the regulation of Pap1-dependent genes could be indirect, mediated by the regulation of Atf1/Pcr1.

Taken together, the above results suggest that under oxidative stress conditions, Flp1 phosphatase is released from the nucleolus to modulate the transcriptional response of the cell. If this was the case, the *flp1-9A-GFP*

mutant, unable to exit the nucleolus in response to 1 mM H₂O₂ treatment, should have a transcriptional response similar to $\Delta flp1$ mutant. Therefore, we next performed qPCR assays to check the expression of several oxidative stress-related genes in both wild-type and $flp1-9A-GFP$ mutant cells under 1 mM H₂O₂ treatment. As shown in Supplementary information Fig. S4, cells expressing $flp1-9A-GFP$ mutant recapitulate the transcriptional profile of $\Delta flp1$ mutant cells for genes such as $atf1^+$, $pcr1^+$, $ctt1^+$, $gpd1^+$, and $srx1^+$.

The increase in the transcriptional response to oxidative stress of $\Delta flp1$ mutant cells correlates with a greater survival.

Deletion of $flp1^+$ seems to have no effect in cell viability when cells grow in solid medium containing 0,6 or 1 mM H₂O₂ (Fig. 1a and²⁹). However, the higher transcriptional induction of all the stress-related genes mentioned above, which combat the harmful effects of oxidative conditions, leads to hypothesize that $\Delta flp1$ mutant cells should be more resistant upon oxidative stress. To delve further into the biological significance of the regulatory role of Flp1 in oxidative stress, we performed survival assays with cells that were first exposed to a low, non-lethal, dose of H₂O₂ to induce basal adaptive response, followed by the incubation with a high dose of the oxidant, that severely compromises growth. After pretreatment with 0.2 mM H₂O₂ for 1 h, only 53% of wild type cells were able to survive a subsequent treatment with 25 mM H₂O₂ for 1 h, while the percentage of survival of $\Delta flp1$ and $flp1-9A-GFP$ cells was 89% and 93% respectively (Fig. 4). This greater survival was even more prominent after 2 h of 25 mM H₂O₂ treatment, time point at which 71% of $\Delta flp1$ cells survived in contrast to only 5% of the wild type. $flp1-9A-GFP$ cells also showed greater survival (16%) than wild type cells although much lower than $\Delta flp1$ ones (Fig. 4). The increased ability to adapt and survive of $\Delta flp1$ cells was also observed when after pretreatment with 0.2 mM H₂O₂ for 1 h, cells were exposed to an intermediate dose of H₂O₂ (2 mM) (Supplementary information Fig. S5a). These data indicate that Flp1 phosphatase is a negative modulator of the adaptive response to H₂O₂, which result in a transient resistance to subsequent higher oxidative stress levels.

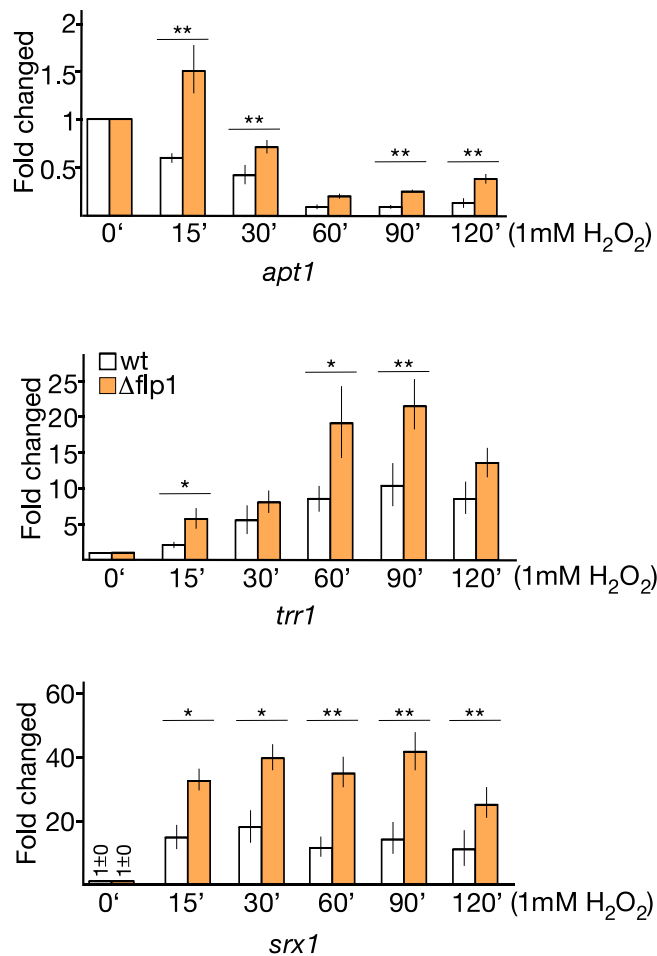


Figure 3. Depletion of Flp1 alters the transcriptional profile of $apt1^+$, $trr1^+$ and $srx1^+$ genes in response to oxidative stress. mRNA levels of $apt1^+$, $trr1^+$ and $srx1^+$ were measured by qPCR from total RNA extracted from wild-type and $\Delta flp1$ strains growing in YES medium containing 1 mM H₂O₂. Total RNAs were prepared from treated cells at the indicated time points. mRNA levels were normalized with ribosomal 18S mRNA and determined with respect to time 0' value, which was considered as 1. Data were expressed as means SD in triplicate. Asterisks indicated statistical significance (*P < 0.05; **P < 0.005, *t*-test unpaired) versus wild-type.

Flp1 phosphatase controls the levels and phosphorylation state of Atf1 and Pcr1 transcription factors upon induction of oxidative stress.

Based on the above results, and given that Atf1 and Pcr1 are phosphoproteins, phosphorylated and dephosphorylated respectively in response to oxidative stress, we then analyzed the dynamics of both the protein levels and the state of phosphorylation of the Atf1/Pcr1 complex upon H_2O_2 treatment in cells lacking *flp1*⁺. Both wild-type and $\Delta flp1$ cells expressing Pcr1-Flag were treated with 1 mM H_2O_2 and protein extracts were obtained throughout time course experiments. Immunoblot analysis using a monoclonal antibody against Atf1 showed that Atf1 levels gradually increased after 30 min H_2O_2 treatment in wild-type cells and that in the absence of *flp1*⁺ this increase was even higher (Fig. 5a). Given that the levels of *atf1* mRNA were upregulated in $\Delta flp1$ cells when compared to wild-type cells, we deduced that these higher Atf1 levels were largely due to the transcriptional upregulation of the *atf1*⁺ gene expression.

Moreover, as shown by immunoblot analysis, a characteristic shift in Atf1 electrophoretic mobility was observed in wild-type cells early after treatment (15 min time point), due to phosphorylation by Sty1³⁹. This shift continued until the 90-min time point, when Atf1 signal began to recover the mobility of its unphosphorylated state (Fig. 5a). In the case of $\Delta flp1$ cells, we observed that the phosphorylation state of Atf1 was similar to that of wild-type cells at early time points (15–30 min). However, unphosphorylated forms were detected earlier (60 min vs 90 min), which is likely to indicate a reduction in the phosphorylation of Atf1 compared to wild-type cells at these time points (Fig. 5a). These data suggest that Sty1-mediated Atf1 phosphorylation is long-term downregulated in the absence of *flp1*⁺. In fact, when testing Sty1 activity in these cells, we unexpectedly found that the dynamics of Sty1 activation during the H_2O_2 treatment decreased earlier in the $\Delta flp1$ mutant compared to wild-type cells (Fig. 5a). Since *pyp2*⁺ mRNA, a negative regulatory member of the SAPK pathway involved in the inhibitory dephosphorylation of Sty1, is also increased in $\Delta flp1$ cells (Fig. 1b), we reasoned that it might be responsible for the faster down-regulation of Sty1. We then analyzed Pyp2 protein levels in both wild-type and $\Delta flp1$ cells by immunoblotting. Indeed, we observed moderately higher levels of Pyp2 in $\Delta flp1$ cells than in the wild-type ones, especially at the last time points (Supplementary information Fig. S6). From these data, we conclude that although the overall magnitude and dynamics of the Sty1-dependent transcriptional response is increased in cells lacking the *flp1*⁺ gene compared to wild-type cells, the long-term result is a faster recovery to pre-stress Sty1 activity levels.

It has been shown that Pcr1, the partner of Atf1 regulating the expression of most of the Sty1-dependent genes under oxidative stress conditions^{15,16} is dephosphorylated upon H_2O_2 treatment¹⁶. Thus, upon oxidative stress, hyperphosphorylation of Atf1 parallels dephosphorylation of Pcr1, both dependent on Sty1 kinase activity¹⁶. Immunoblot assays allowed us to corroborate previous findings regarding the accumulation of Pcr1 protein upon H_2O_2 -mediated oxidative stress⁴⁰, which was higher in $\Delta flp1$ cells, correlating with the higher levels of *pcr1* mRNA in $\Delta flp1$ cells compared to wild-type ones under these stress conditions (Fig. 2a). Interestingly, in cells lacking Flp1 phosphatase, Pcr1 never reached the dephosphorylation level observed in wild-type cells, even its phosphorylated forms were the most predominant at the later time points analyzed during the H_2O_2 treatment (Fig. 5b). These data suggest that Flp1 could be, at least in part, the phosphatase responsible for Pcr1 dephosphorylation under oxidative stress conditions.

It has been reported that Atf1 stability is modulated by Sty1 phosphorylation and binding with Pcr1⁴⁰. Since phosphorylation status of Atf1 in $\Delta flp1$ cells differs from that of wild-type ones at later time points, when it appears less phosphorylated (Fig. 5a), and based on the fact that Pcr1 shows increased phosphorylation in the absence of Flp1, we studied whether the higher Atf1 levels in $\Delta flp1$ cells are due to its interaction with Pcr1. As

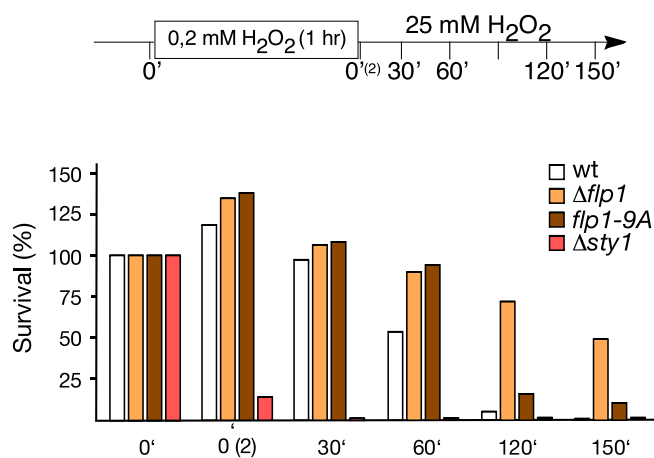


Figure 4. $\Delta flp1$ cells display greater resistance to acute oxidative stress conditions after exposure to an adaptation period. Asynchronous cultures of indicated strains growing at 30 °C in YES were incubated with 0.2 mM of H_2O_2 during 1 h. Then, cells were stressed with 25 mM H_2O_2 . Cell viability was measured at the indicated time points by plating appropriate dilution of cells onto YES agar plates. The number of viable cells was measured after 3 days incubation at 30 °C. Viability is expressed as a percentage of the number of colonies obtained before the addition of the first dose of H_2O_2 . Experiment was repeated twice (see Supplementary Information Fig. S5b), and a representative experiment is shown.

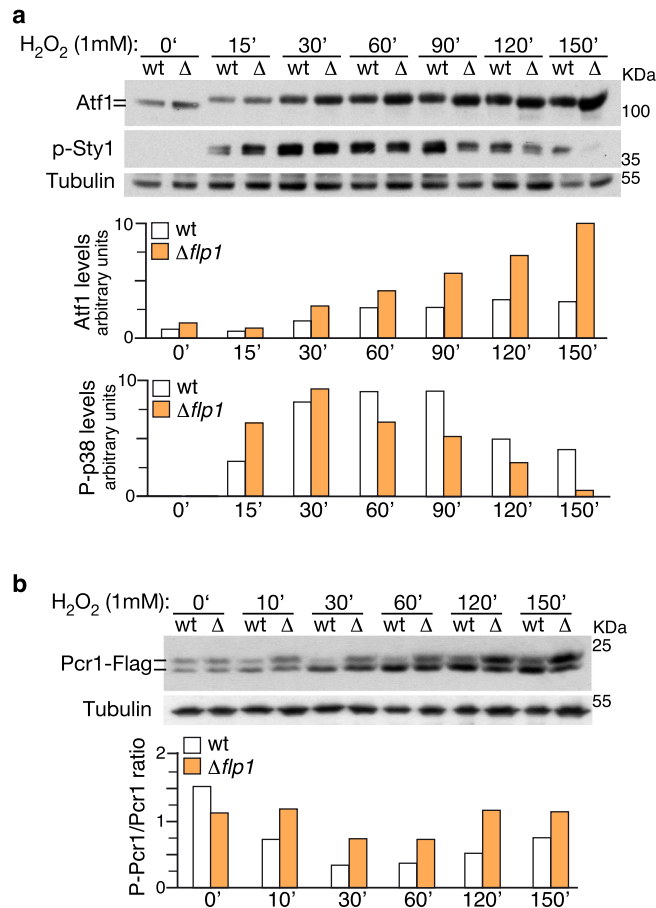


Figure 5. Protein levels and phosphorylation states of Atf1 and Pcr1 transcription factors upon oxidative stress induction. **(a,b)** Wild-type and $\Delta flp1$ cells (Δ) expressing a Pcr1-Flag fusion protein were grown in YES medium to mid-log phase and treated with 1 mM H₂O₂ for the indicated times. Total extracts were resolved by SDS-PAGE and analyzed by Western blot. **(a)** Atf1 was detected by incubation with a monoclonal anti-Atf1 antibody. Activated Sty1 was detected with anti-phospho-p38 antibody. Tubulin was used as loading control. Normalization of quantified Atf1 and activated Sty1 are shown in bar diagrams. Results from a representative experiment are shown. Blot membranes were cut prior antibodies incubation (Supplementary information Fig. S10). **(b)** Pcr1 was detected by incubation with anti-Flag antibody. Tubulin was used as loading control. Phospho-Pcr1/dephospho-Pcr1 ratios are shown in bar diagrams. Results from a representative experiment are shown. Full-length blots are shown in Supplementary Fig. S10.

shown in Fig. 6, the higher increase of both protein and mRNA Atf1 levels, observed in $\Delta flp1$ cells under oxidative stress conditions, was abolished in the double mutant $\Delta flp1 \Delta pcr1$, indicating that Atf1 abnormalities observed in $\Delta flp1$ cells are mediated by Pcr1.

Flp1 interacts with and dephosphorylates the transcription factor Pcr1. To investigate whether Flp1 directly regulates the phosphorylation state of Pcr1 in response to oxidative stress, we first analyzed whether Flp1 and Pcr1 proteins interact *in vivo*. We exposed cell cultures to 1 mM H₂O₂ and immunoprecipitated Pcr1-Flag tagged protein from a strain also expressing Flp1 protein tagged with the HA epitope. The interaction was also checked in untreated cells. To preserve the characteristic labile interactions between phosphatases and their substrates, as well as Atf1-Pcr1 complexes, we used formaldehyde to cross-link protein complexes in cultured cells. Immunoprecipitated Flag-Pcr1 was resolved by SDS-PAGE gels followed by immunoblotting with the corresponding antibodies. Flp1 was clearly detected in the Flag-Pcr1 immunoprecipitates obtained from cells treated with H₂O₂ (Fig. 7a), indicating that Flp1 interacts with Pcr1 under oxidative stress conditions.

Finally, to examine whether Pcr1 is a direct substrate of Flp1, we performed *in vitro* phosphatase assays using Pcr1-Flag immunoprecipitates obtained from exponentially cells grown in YES medium and recombinant GST-Flp1 or GST-Flp1-CS (a catalytically inactive form) fusion proteins purified from the proper *S. pombe* strains. As shown in Fig. 7b, incubation of Pcr1-Flag immunoprecipitates with λ -PPase, used as a positive control, and wild-type Flp1, but not with the catalytically inactive GST-Flp1-CS form, resulted in some degree of Pcr1 dephosphorylation, as shown by the reduction level of the phosphorylated Pcr1 upper band (Fig. 7c), indicating that Flp1 is able to dephosphorylate Pcr1 *in vitro*. All these data support a role for Flp1 in the dephosphorylation of Pcr1 during oxidative stress.

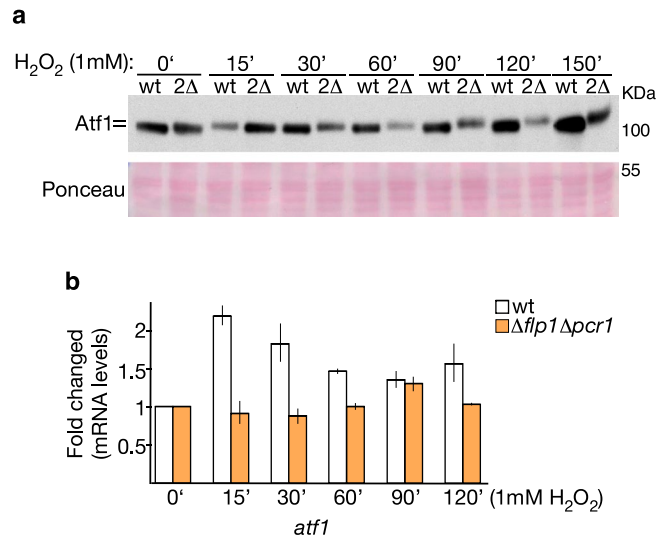


Figure 6. Protein and mRNA levels of Atf1 transcription factor in cells lacking both *flp1* and *pcr1* genes upon oxidative stress induction. **(a,b)** Wild-type and $\Delta flp1 \Delta pcr1$ mutant cells (2Δ) were grown in YES medium to mid-log phase and treated with 1 mM H₂O₂ at the indicated time points. **(a)** Total protein extracts were resolved by SDS-PAGE and analyzed by Western blot. Atf1 was detected by incubation with a monoclonal anti-Atf1 antibody. Ponceau staining was used as loading control. Full-length blots are shown in Supplementary Fig. S12. **(b)** Total RNAs were prepared from untreated (0') and treated cells at the time points indicated. mRNA levels of *atf1*⁺ were measured by qPCR, normalized against ribosomal 18S mRNA and determined with respect to time 0' values, which were considered as 1. Data represent the average of two biological replicates.

Discussion

Eukaryotic cells are continuously exposed to ROS during normal aerobic metabolism. However, an excess of ROS causes oxidative stress by damaging all cellular components including DNA, proteins, and lipids. Cells have developed response mechanisms to avoid these harmful effects, maintain ROS homeostasis and maximize survival. One of the major signaling pathways, SAPK pathway, reprograms gene expression to induce proteins with stress protection function. In *S. pombe*, Sty1 MAPK, the p38 kinase ortholog in mammals, is activated to stimulate gene expression via the Atf1 transcription factor which is closely related to ATF2 in humans¹⁸. Sty1-mediated phosphorylation of Atf1 is essential to promote transcription initiation¹¹. Atf1 forms a heterodimer with the transcription factor Pcr1, also a basic zipper (bZIP) protein, which seems to allow proper recognition of Atf1-binding sites at most promoters¹¹. Pcr1 is also a phosphoprotein that is specifically dephosphorylated in a Sty1-dependent manner under oxidative stress¹⁶, although the functional meaning of this posttranscriptional modification is still unknown. Moreover, the pathway driven by the bZIP transcription factor Pap1 is also involved in the cellular response to oxidative stress²¹. Pap1 contributes with Atf1-Pcr1 to properly activate essential antioxidant genes and, in turn to get a full transcriptional response^{11, 22, 23, 41}.

The conserved Cdc14 phosphatase family, implicated in the reversal of Cdk and MAPK substrate phosphorylation to regulate cell cycle progression in yeast^{42–44}, is also involved in the response to different types of cellular stress. Moreover, it has been described that the *S. pombe* Cdc14 ortholog, Flp1, whose activity is largely controlled by subcellular location, participates in the cellular response to replicative stress²⁸. Thus, by exiting its interphase nucleolar localization and its subsequent accumulation in the nucleoplasm, Flp1 contributes to the full activation of the replicative stress checkpoint²⁸. One mammalian ortholog, Cdc14B, also responds to DNA damage insults exiting the nucleolus to participate in the DNA damage checkpoint activation⁴⁵. Moreover, it has been shown that Flp1 also responds to oxidative stress conditions by exiting the nucleolus and accumulating in the nucleoplasm²⁹, although the biological meaning of this localization change is not yet understood. Nonetheless, we report here that Flp1 phosphatase modulates the transcriptional response to oxidative stress, likely acting on the Atf1/Pcr1 transcriptional complex.

Although the lack of *flp1*⁺ in *S. pombe* does not sensitize cells to oxidative stress caused by the continuous exposure to intermediate doses of H₂O₂ treatment (this work and²⁹), we found that the sensitivity of stress-activated MAPKs mutants, such as $\Delta wis1$ and $\Delta sty1$, to oxidative stress caused by H₂O₂ treatment, is partially suppressed when combined with $\Delta flp1$. Moreover, we also found that both $\Delta flp1$ and *flp1-9A-GFP* mutant cells survive better than wild-type cells when exposed to acute oxidative stress after pretreatment with low, non-lethal, doses of H₂O₂ to allow cells to adapt the response.

This suggests that Flp1 phosphatase plays a role in the regulation of the oxidative stress response, likely acting as a negative modulator of the adaptive response to low levels of ROS in the cellular environment.

It has been reported that the active release of Flp1 phosphatase from the nucleolus to the nucleoplasm is an all-or-none response mediated by the phospho-dependent association of Rad24 with the phosphatase, which avoids returning to the nucleolus upon those environmental conditions. In this scenario, Pmk1/Cdk1 kinases preferentially acting upon oxidative stress²⁹, and Cds1/Chk1 the ones that phosphorylate Flp1 in response to

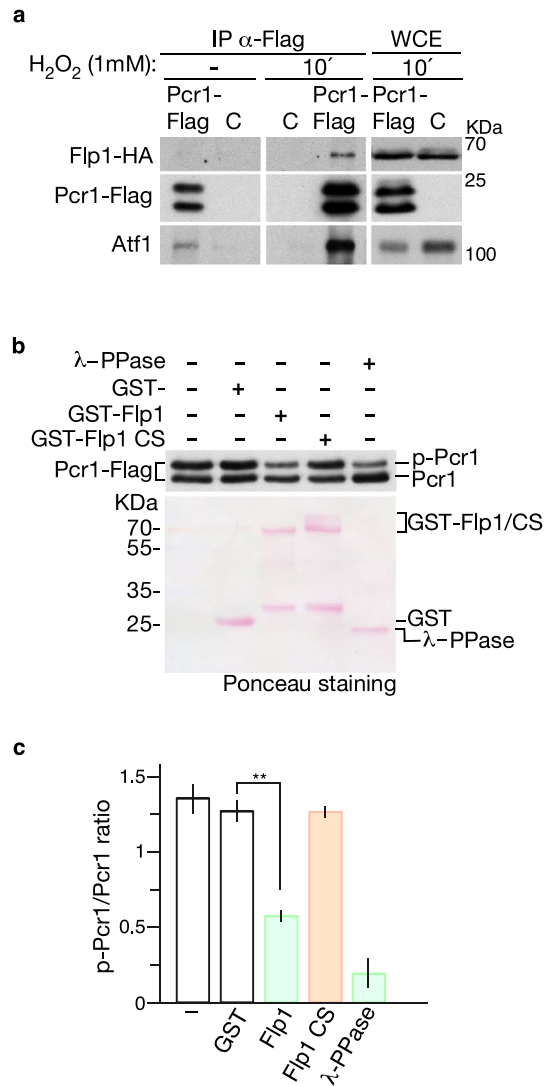


Figure 7. Pospho-Pcr1 protein is a substrate of Flp1 phosphatase. **(a)** Coimmunoprecipitation of Pcr1-Flag and Flp1-HA fusion protein from yeast extracts obtained from indicated strains untreated or treated with 1 mM H₂O₂ for 10 min and incubated with formaldehyde for 20 min before processing. Anti Flag antibody was used to immunoprecipitate Pcr1-Flag fusion protein. Immunoprecipitates were analyzed by immunoblot using anti-Flag, anti-HA and anti-Atf1 antibodies. *IP* immunoprecipitation, *WCE* whole cell extracts; C, negative control: untagged strain. Cropped gels are shown. Unprocessed original scans of blots, cut prior antibodies incubation, are shown in Supplementary information Fig. S13. **(b)** Flp1 dephosphorylates Pcr1 in vitro. Pcr1-FLAG was immunoprecipitated from protein extracts prepared from $\Delta flp1$ cells treated with 1 mM H₂O₂ for 10 min. After washing, Pcr1-FLAG immunoprecipitates were incubated with GST-Flp1, the phosphatase dead mutant GST-Flp1-CS, GST alone or λ phosphatase. Samples were resolved by SDS-PAGE and detected by immunoblot with anti-FLAG antibody or ponceau staining. Full-length blots are shown in Supplementary Fig. S13. **(c)** Quantification of in vitro phosphatase assays performed as described in **(b)**. Bars (Phospho-Pcr1/dephospho-Pcr1 ratio) indicate the average from four independent experiments. ** $P < 0.005$, as calculated by unpaired Student's *t* test.

replicative stress^{28,29}. However, by using a previously characterized Flp1 mutant, in which all nine Cds1/Chk1-mediated RxxS phosphosites were eliminated (Flp1-9A-GFP)²⁸, we found that Cds1/Chk1-related kinases seem also to underlie the nuclear accumulation of the phosphatase in response to oxidative stress. Previous accurate studies have shown that abolishing six Flp1 RxxS phosphosites, although significantly hampered Flp1 nucleoplasmic accumulation, was not enough to fully prevent Flp1 release from the nucleolus under H₂O₂ treatment, and that this required three additional mutations at the putative Pmk1/Cdk1-dependent TP phosphosites present in Flp1 (Flp1-6A3A-GFP mutant). These observations strongly suggested that phosphorylation of Flp1 at both RxxS and TP sites regulates its relocalization from the nucleolus to the nucleoplasm upon oxidative stress²⁹. Additionally, this difference in reported data could be due to the alteration of Cdk/Pmk1-mediated Flp1 phosphorylation sites as a consequence of conformational changes of Flp1 resulting from the nine serine mutations in

the Flp1-9A-GFP mutant. However, the fact that Flp1-9A-GFP cells behave as wild-type cells in an unperturbed cell cycle²⁸ supports the former postulate.

Several Sty1-dependent mechanisms have been suggested to explain the increase of *atf1*⁺ expression levels in response to stress. This high levels of Atf1 are important for proper adaptation to maximize cell survival under these harmful conditions but not for unstressed cells^{40, 46–48}, indicating that normal expression levels of *atf1*⁺ have to be recovered even under persistent stress. Similar to *atf1*⁺, the Atf1-mediated increase in the expression of genes with a stress-protective function decay after a certain time until reaching their characteristic levels of unstressed conditions. Under oxidative stress, lack of Flp1 phosphatase results in a significant increase in the transcription levels of Sty1/Atf1-dependent genes when compared with the levels reached in wild-type cells. Moreover, in $\Delta flp1$ cells, this transcriptional response is also deregulated in time. Thus, $\Delta flp1$ cells respond by a significant higher transcriptional induction, in both magnitude and duration, of key genes such as *ctt1*⁺, *gpd1*⁺, *hsp9*⁺ and *pyp2*⁺ compared to wild-type cells. Analysis of *atf1*⁺ and *pcr1*⁺ induction also showed longer transcriptional kinetics over time, in which the mRNA levels prior to stress were not recovered during the time the analysis lasted. The upregulation of *atf1*⁺ and *pcr1*⁺ transcription factors in $\Delta flp1$ cells most likely account for the upregulation of the stress-activated genes presented in this work. Moreover, upregulation of Pap1-dependent genes in response to oxidative stress was also higher in $\Delta flp1$ cells when comparing with wild-type ones.

Upon the induction of oxidative stress, the lack of Flp1 also results in a significant increase in Atf1 and Pcr1 protein levels, most likely reflecting the also higher *atf1*⁺ and *pcr1*⁺ mRNA levels, an anomalous phosphorylation state of both transcription factors, and intriguingly, a faster deactivation of the Sty1 kinase. Sty1-mediated phosphorylation of Atf1 has a key effect on the stress-activated transcriptional response by establishing proper interactions with the basal transcriptional machinery for transcription initiation¹¹. In $\Delta flp1$ cells, the oxidative stress-dependent phosphorylation of Atf1 is similar to that observed in wild-type cells, although dephosphorylated forms are detected earlier in time, which may reflect the earlier deactivation of Sty1 in $\Delta flp1$ cells, most likely due to the higher levels of Pyp2 phosphatase reached at the later time points in these cells as compared to wild-type ones. Parallel to Atf1 phosphorylation, Pcr1 is dephosphorylated upon oxidative stress conditions¹⁶. Remarkably, Pcr1 dephosphorylation is much less evident in cells lacking Flp1. Since Pcr1 is dephosphorylated in a Sty1-dependent manner, the faster deactivation of Sty1 in $\Delta flp1$ cells could also account for the predominance of phosphorylated forms of Pcr1 at later time points. However, the lack of Pcr1 dephosphorylation in $\Delta flp1$ cells at early time points cannot be explained as a consequence of the downregulation of Sty1 activity. An attractive possibility is that Flp1 modulates the response to oxidative stress, interacting with and dephosphorylating stress-regulated transcription factors. Several lines of evidence shown here strongly suggest that this is the case. First, in cells lacking *flp1*⁺, transcription of Sty1-Atf1-mediated oxidative stress genes is deregulated. Second, Flp1 associates in vivo with the Pcr1-Atf1 complex under oxidative stress conditions. Third, Flp1 dephosphorylates the Atf1-cofactor Pcr1 in vitro and the absence of Flp1 correlates with the lack of Pcr1 dephosphorylation in vivo in response to oxidative stress. Lastly, when we checked cell viability in response to H₂O₂ treatment in both $\Delta pcr1$ and $\Delta pcr1 \Delta flp1$ mutants we did not observe additive effects (Supplementary Fig. S7), suggesting that the two proteins work in the same pathway.

Previous works have already reported a role for Flp1 in the transcriptional regulation of genes important for mitosis and cytokinesis as well as S phase gene expression, most likely through the association and dephosphorylation of specific transcription factors^{49, 50}. Moreover, mammalian Cdc14 paralogs have also been involved in transcriptional regulation. Thus, the mouse Cdc14B paralog, in pluripotent cells, regulates the exit from stemness to differentiation through dephosphorylation and consequent degradation of the UTF1 repressor transcription factor⁵¹. In addition, the human Cdc14B phosphatase participates in the repression of cell cycle transcription by direct RNA polymerase II regulation⁵².

Our data support a model in which Flp1 is released from the nucleolus to the nucleoplasm upon oxidative stress through the phosphorylation of its RxxS phosphosites and the consequent association of Flp1 with Rad24. Once released, nuclear Flp1 phosphatase, bound or not to Rad24, interacts with the Atf1/Pcr1 complex, dephosphorylating Pcr1 to modulate the transcriptional response. Flp1 may be involved in the dephosphorylation of Pcr1 in combination with other unknown phosphatases, but it could be also acting on another not yet known target, such as Pap1 itself (Fig. 8). Therefore, we propose that Flp1-phosphatase is a negative regulator of the transcriptional response to oxidative stress acting on its deactivation or maintaining the activity levels of the Wis1/Sty1 pathway within certain limits. How the dephosphorylation of Pcr1 by Flp1 underlies the modulation of the transcriptional response and to understand whether Pap1 is regulated by Flp1 will be subjects of future studies.

Material and methods

Fission yeast strains, growth conditions and media. The strains used in this study are listed in Supplementary information Table S1. Media and genetic methods for studying fission yeast were previously described⁵³. For plate survival assays, serial dilutions of exponentially growing cultures of strains indicated were plated in media without or with different concentrations of H₂O₂ (as indicated in figure legends). Plates were incubated at 30 °C for three days and then scanned.

Plasmids construction. Plasmids pRepKZ-*flp1*⁺ complete ORFs under the *nmt1* promoter was constructed by PCR amplification from genomic DNA. Transformation was performed by lithium acetate protocol or electroporation and transformants were selected by growing in selective medium.

RNA analysis. RNA samples for Northern analysis were prepared from 0.5 × 10⁹ cells. Yeast cultures grown at 30 °C to early log phase were kept untreated or exposed to 1 mM H₂O₂ for the time specified in the figure legends. Pellets were resuspended in 200 ml RNA extraction buffer (0.1 M EDTA pH 8.0, 0.1 M NaCl, 50 mM

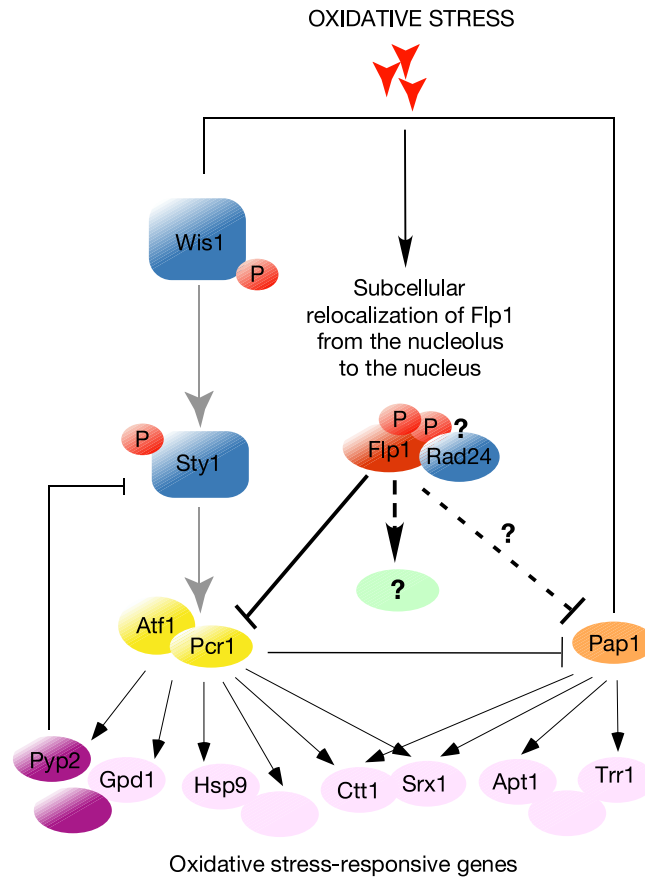


Figure 8. Model of the role of Flp1/Cdc14 in the modulation of the transcriptional response to oxidative stress (See text for details).

Tris pH 8.0) with 200 ml Phenol/Chloroform and 5 ml 10% SDS. Cells were disrupted with glass-beads in a Fast-prep and then spined in a microfuge for 15 min. The aqueous layer was collected and extracted once with Phenol, three times with Phenol/Chloroform and once with Chloroform/Isoamyl alcohol. RNA was precipitated with sodium acetate and isopropanol. RNA pellets were then washed with 70% Ethanol and resuspended in H₂O. Total RNA (6 µg) was denatured by heating at 70 °C and deionized formamide and formaldehyde was added to each sample. Samples were separated in Formaldehyde 1.2% agarose with ethidium bromide gels and transferred to a Hybond-N membrane (GE Healthcare). 500 nucleotides gene specific probes were obtained by PCR amplification from genomic DNA and labelled with ³²P-α-dCTP. Transcript levels were quantified according to loading control using Bio-Rad Molecular Personal FX Phosphorimager. For quantitative real-time PCR (qPCR) analysis, total RNAs were purified using the RNeasy minikit (Qiagen), treated with DNase (Invitrogen) and quantified using a NanoDrop spectrophotometer (Isogen). Total RNAs (1 µg) were reversed transcribed into cDNA using iScript reverse transcription supermix (Bio-Rad). qPCRs were performed using the iTaq Universal SYBR green supermix and an iCycler PCR system (Bio-Rad). Relative gene expression was normalized using a stress-independent gene (18S rRNA). Gene specific primers used for qPCRs are indicated in Supplementary information Table S2.

For distinguishing between mRNA synthesis or mRNA stability cells were grown to OD₆₀₀ of 0.4 and then 1,10-phenanthroline dissolved in ethanol was added to cultures (250 µg/ml) to inhibit transcription.

Protein methods. Western blotting analysis. Whole cell extracts were prepared by precipitation with trichloroacetic acid (TCA). *S. pombe* strains were grown in YES medium to OD₆₀₀ of 0.4–0.5 and cells (5 ml) were collected by centrifugation just after the addition of 100% TCA to a final concentration of 10% and washed in 20% TCA. Cell disruption was performed with Glass-Beads in a Fast-Prep and 12.5% TCA. Cell lysates were pelleted by centrifugation at 3,000 rpms and resuspended in 1X LB loading buffer and Tris base. Samples were electrophoretically resolved by SDS-PAGE and transferred to Nitrocellulose membranes using a Bio-Rad transfer unit. Blots were then probed against antibodies indicated. Antibodies used: monoclonal anti-Atf1 (Abcam), anti-HA-HRP conjugated (Miltenyi Biotec), anti-Flag-HRP conjugated (Sigma), anti-Myc-HRP conjugated (Miltenyi Biotec), anti phospho-p38 MAP Kinase (Cell Signaling) and anti-α-tubulin (Sigma-Aldrich).

Coimmunoprecipitation. For immunoprecipitation of Flag-tagged Pcr1 protein, *S. pombe* strains expressing Pcr1-Flag and/or Flp1-HA fusion proteins were grown in YES at 30 °C to an OD₆₀₀ of 0.5. Then H₂O₂ (1 mM) was added to part of the cultures and after 10 min incubation formaldehyde (1.5% vol/vol) was added for 30 min at room temperature. Cells were pelleted and washed three times with ice cold TBS. Pellets were resuspended in 500 ml lysis buffer (20 mM Tris, pH 8, 100 mM NaCl, 2 mM EDTA and 0.5% NP-40) supplemented with a protease inhibitor cocktail (Complete, EDTA-free, Sigma-Aldrich) and disrupted with Glass-Beads in a Fast-Prep. Cell lysates were clarified by centrifugation at 13,000 rpm and protein concentration was determined using BCA Protein Assay kit (Pierce Chemical, Rockford, IL). Cell extracts (3 mg) were incubated with dynabeads protein G (Invitrogen) bound to monoclonal anti-Flag antibody (Agilent Technologies) for 5 h at 4 °C. Beads were washed four times with lysis buffer and resuspended in loading buffer. Immunoprecipitates were resolved by SDS-PAGE, transferred to Nitrocellulose membranes using a Bio-Rad transfer unit and analyzed with anti-HA-HRP conjugated (Miltenyi Biotec), anti-Flag-HRP conjugated (Sigma) and anti-Atf1 (Abcam) antibodies.

In vitro phosphatase assays. Pcr1-Flag was immunoprecipitated from cells grown in YES at 30 °C to an OD₆₀₀ of 0.5. Cells were recovered by centrifugation, disrupted with Glass-Beads in the mentioned buffer lysis, and immunoprecipitation was performed as described above. GST-Flp1 and GST-Flp1-CS fusion proteins were purified from *S. pombe* strains containing the corresponding repressible *nmt1*-plasmids. Cells were grown in minimal medium appropriately supplemented (adenine and uracil) and containing thiamine until exponential phase. Induction was performed by washing cells three times with water and inoculated on minimal medium without thiamine at OD₆₀₀ of 0.05. Cultures were allowed to grow at 30 °C for 16 h. GST-Flp1 fusion proteins were purified from these cells as previously described (Díaz-Cuervo 2008). Pcr1-Flag immunoprecipitates were washed in phosphatase buffer (50 mM Imidazol pH 7, 1 mM EDTA, 1 mM DTT) and incubated for 30 min at 30 °C with GST-Flp, GST-Flp1-CS, GST- alone or λ-phosphatase in the above phosphatase buffer. Reactions were stopped by addition of loading buffer and boiling for 5 min at 95 °C. Proteins were resolved by SDS-PAGE, transferred to nitrocellulose membranes and analyzed with anti-Flag-HRP conjugated antibody to detect Pcr1-Flag mobility. Membranes were also analyzed by ponceau staining to detect GST- fusion proteins.

Mycroscopy. GFP-, EGFP-, mCherry-, and RFP-tagged strains were grown in YES medium until exponential phase. 1 mM H₂O₂ was added during 1 h and the presence of specific fluorescence was detected by fluorescence microscopy using a Thunder Imager (camera, DFC9000; Leyca) microscope.

Data availability

The datasets supporting the current study are available from the corresponding authors on request.

Received: 12 January 2023; Accepted: 1 September 2023

Published online: 06 September 2023

References

1. Veal, E. A., Day, A. M. & Morgan, B. A. Hydrogen peroxide sensing and signaling. *Mol. Cell* **26**, 1–14. <https://doi.org/10.1016/j.molcel.2007.03.016> (2007).
2. Millar, J. B. A., Buck, V. & Wilkinson, M. G. Pyp1 and Pyp2 PTPases dephosphorylate an osmosensing MAP kinase controlling cell size at division in fission yeast. *Genes Dev.* **9**, 2117–2130. <https://doi.org/10.1101/gad.9.17.2117> (1995).
3. Degols, G., Shiozaki, K. & Russell, P. Activation and regulation of the Spc1 stress-activated protein kinase in *Schizosaccharomyces pombe*. *Mol. Cell Biol.* **16**, 2870–2877. <https://doi.org/10.1128/MCB.16.6.2870> (1996).
4. Wilkinson, M. G. *et al.* The Atf1 transcription factor is a target for the Sty1 stress-activated MAP kinase pathway in fission yeast. *Genes Dev.* **10**, 2289–2301. <https://doi.org/10.1101/gad.10.18.2289> (1996).
5. Shiozaki, K., Shiozaki, M. & Russell, P. Heat stress activates fission yeast Spc1/Sty1 MAPK by a MEKK-independent mechanism. *Mol. Biol. Cell* **9**, 1339–1349. <https://doi.org/10.1091/mbc.9.6.1339> (1998).
6. Jang, M. J., Jwa, M., Kim, J. H. & Song, K. Selective inhibition of MAPKK Wis1 in the stress-activated MAPK cascade of *Schizosaccharomyces pombe* by novel berberine derivatives. *J. Biol. Chem.* **277**, 12388–12395. <https://doi.org/10.1074/jbc.M111018200> (2002).
7. Nguyen, A. N., Ikner, A. D., Shiozaki, M., Warren, S. M. & Shiozaki, K. Cytoplasmic localization of Wis1 MAPKK by nuclear export signal is important for nuclear targeting of Spc1/Sty1 MAPK in fission yeast. *Mol. Biol. Cell* **13**, 2651–2663. <https://doi.org/10.1091/mbc.02-03-0043> (2002).
8. Shieh, J. C. *et al.* The Mcs4 response regulator coordinately controls the stress-activated Wak1-Wis1-Sty1 MAP kinase pathway and fission yeast cell cycle. *Genes Dev.* **11**, 1008–1022. <https://doi.org/10.1101/gad.11.8.1008> (1997).
9. Samejima, I., Mackie, S., Warbrick, E., Weisman, R. & Fantès, P. A. The fission yeast mitotic regulator win1 encodes an MAP kinase kinase that phosphorylates and activates Wis1 MAP kinase kinase in response to high osmolarity. *Mol. Biol. Cell* **9**, 2325–2335. <https://doi.org/10.1091/mbc.9.8.2325> (1998).
10. Shieh, J. C., Wilkinson, M. G. & Millar, J. B. A. The Win1 mitotic regulator is a component of the fission yeast stress-activated Sty1 MAPK pathway. *Mol. Biol. Cell* **9**, 311–322. <https://doi.org/10.1091/mbc.9.2.311> (1998).
11. Salat-Canela, C. *et al.* Deciphering the role of the signal- and Sty1 kinase-dependent phosphorylation of the stress-responsive transcription factor Atf1 on gene activation. *J. Biol. Chem.* **292**, 13635–13644. <https://doi.org/10.1074/jbc.M117.794339> (2017).
12. Sánchez-Mir, L. *et al.* Phospho-mimicking Atf1 mutants bypass the transcription activating function of the MAP kinase Sty1 of fission yeast. *Curr. Genet.* **64**, 97–102. <https://doi.org/10.1007/s00294-017-0730-7> (2018).
13. Takeda, T. *et al.* *Schizosaccharomyces pombe* atf1+ encodes a transcription factor required for sexual development and entry into stationary phase. *EMBO J.* **14**, 6193–6208. <https://doi.org/10.1002/j.1460-2075.1995.tb00310.x> (1995).
14. Degols, G. & Russell, P. Discrete roles of the Spc1 kinase and the Atf1 transcription factor in the UV response of *Schizosaccharomyces pombe*. *Mol. Cell Biol.* **17**, 3356–3363. <https://doi.org/10.1128/MCB.17.6.3356> (1997).
15. Eshaghi, M. *et al.* Genomic binding profiling of the fission yeast stress-activated MAPK sty1 and the bZIP transcriptional activator Atf1 in response to H₂O₂. *PLoS ONE*. **5**, e11620. <https://doi.org/10.1371/journal.pone.0011620> (2010).
16. Sansó, M., Gogol, M., Ayté, J., Seidel, C. & Hidalgo, E. Transcription factors Pcr1 and Atf1 have distinct roles in stress- and Sty1-dependent gene regulation. *Eukaryot. Cell*. **7**, 826–835. <https://doi.org/10.1128/EC.00465-07> (2008).

17. Kyriakis, J. M. & Avruch, J. Mammalian MAPK signal transduction pathways activated by stress and inflammation: A 10-year update. *Physiol. Rev.* **92**, 689–737. <https://doi.org/10.1152/physrev.00028.2011> (2012).
18. Shiozaki, K. & Russell, P. Cell-cycle control linked to extracellular environment by MAP kinase pathway in fission yeast. *Nature* **378**, 739–743. <https://doi.org/10.1038/378739a0> (1995).
19. Samejima, I., Mackie, S. & Fantès, P. A. Multiple modes of activation of the stress-responsive MAP kinase pathway in fission yeast. *EMBO J.* **16**, 6162–70. <https://doi.org/10.1093/emboj/16.20.6162> (1997).
20. Di, Y. *et al.* H₂O₂ stress-specific regulation of *S. pombe* MAPK Sty1 by mitochondrial protein phosphatase Ptc4. *EMBO J.* **31**, 563–75. <https://doi.org/10.1038/emboj.2011.438> (2012).
21. Toone, W. M. *et al.* Regulation of the fission yeast transcription factor Pap1 by oxidative stress: Requirement for the nuclear export factor Crm1 (Exportin) and the stress-activated MAP kinase Sty1/Spcl. *Genes Dev.* **12**(10), 1453–1463. <https://doi.org/10.1101/gad.12.10.1453> (1998).
22. Quinn, J. *et al.* Distinct regulatory proteins control the graded transcriptional response to increasing H₂O₂ levels in fission yeast *Schizosaccharomyces pombe*. *Mol. Biol. Cell* **13**, 805–816. <https://doi.org/10.1091/mbc.01-06-0288> (2002).
23. Chen, D. *et al.* Multiple pathways differentially regulate global oxidative stress responses in fission yeast. *Mol. Biol. Cell* **19**, 308–317. <https://doi.org/10.1091/mbc.e07-08-0735> (2008).
24. Cueille, N. *et al.* Flp1, a fission yeast orthologue of the *S. cerevisiae* CDC14 gene, is not required for cyclin degradation or rum1p stabilisation at the end of mitosis. *J. Cell Sci.* **114**, 2649–64. <https://doi.org/10.1242/jcs.114.14.2649> (2001).
25. Trautmann, S. *et al.* Fission yeast Clp1p phosphatase regulates G₂/M transition and coordination of cytokinesis with cell cycle progression Background. In *Saccharomyces cerevisiae* the mitotic-exit network (MEN). *Curr. Biol.* **11**, 931–40. [https://doi.org/10.1016/s0960-9822\(01\)00268-8](https://doi.org/10.1016/s0960-9822(01)00268-8) (2001).
26. Esteban, V. *et al.* A role for the Cdc14-family phosphatase Flp1p at the end of the cell cycle in controlling the rapid degradation of the mitotic inducer Cdc25p in fission yeast. *J. Cell Sci.* **117**, 2461–2468. <https://doi.org/10.1242/jcs.01107> (2004).
27. Wolfe, B. A. & Gould, K. L. Fission yeast Clp1p phosphatase affects G₂/M transition and mitotic exit through Cdc25p inactivation. *EMBO J.* **23**, 919–929. <https://doi.org/10.1038/sj.emboj.7600103> (2004).
28. Díaz-Cuervo, H. & Bueno, A. Cds1 controls the release of Cdc14-like phosphatase Flp1 from the nucleolus to drive full activation of the checkpoint response to replication stress in fission yeast. *Mol. Biol. Cell* **19**, 2488–2499. <https://doi.org/10.1091/mbc.E07-08-0737> (2008).
29. Broadus, M. R. & Gould, K. L. Multiple protein kinases influence the redistribution of fission yeast Clp1/Cdc14 phosphatase upon genotoxic stress. *Mol. Biol. Cell* **23**, 4118–4128. <https://doi.org/10.1091/mbc.E12-06-0475> (2012).
30. Chen, D. *et al.* Global transcriptional responses of fission yeast to environmental stress. *Mol. Biol. Cell* **14**, 214–229. <https://doi.org/10.1091/mbc.e02-08-0499> (2003).
31. Smith, D. A. *et al.* The Srk1 protein kinase is a target for the Sty1 stress-activated MAPK in fission yeast. *J. Biol. Chem.* **277**, 33411–33421. <https://doi.org/10.1074/jbc.M204593200> (2002).
32. López-Avilés, S. *et al.* Inactivation of the Cdc25 phosphatase by the stress-activated Srk1 kinase in fission yeast. *Mol. Cell* **17**, 49–59. <https://doi.org/10.1016/j.molcel.2004.11.043> (2005).
33. Davidson, M. K., Shandilya, H. K., Hirota, K., Ohta, K. & Wahls, W. P. Atf1-Pcr1-M26 complex links stress-activated MAPK and cAMP-dependent protein kinase pathways via chromatin remodeling of *cgs2*. *J. Biol. Chem.* **279**, 50857–50863. <https://doi.org/10.1074/jbc.M409079200> (2004).
34. Fernández-Vázquez, J. *et al.* Modification of tRNALysUUU by elongator is essential for efficient translation of stress mRNAs. *PLoS Genet.* **9**, e1003647. <https://doi.org/10.1371/journal.pgen.1003647> (2013).
35. Grigull, J., Mnaimneh, S., Pootoolal, J., Robinson, M. D. & Hughes, T. R. Genome-wide analysis of mRNA stability using transcription inhibitors and microarrays reveals posttranscriptional control of ribosome biogenesis factors. *Mol. Cell Biol.* **24**, 5534–5547. <https://doi.org/10.1128/MCB.24.12.5534-5547.2004> (2004).
36. Mutoh, N., Nakagawa, C. W. & Yamada, K. Characterization of Cu, Zn-superoxide dismutase-deficient mutant of fission yeast *Schizosaccharomyces pombe*. *Curr. Genet.* **41**, 82–88. <https://doi.org/10.1007/s00294-002-0288-9> (2002).
37. Vivancos, A. P., Castillo, E. A., Jones, N., Ayté, J. & Hidalgo, E. Activation of the redox sensor Pap1 by hydrogen peroxide requires modulation of the intracellular oxidant concentration. *Mol. Microbiol.* **52**, 1427–1435. <https://doi.org/10.1111/j.1365-2958.2004.04065> (2004).
38. Vivancos, A. P. *et al.* A cysteine-sulfinic acid in peroxiredoxin regulates H₂O₂-sensing by the antioxidant Pap1 pathway. *Proc. Natl. Acad. Sci. USA* **102**, 8875–8880. <https://doi.org/10.1073/pnas.0503251102> (2005).
39. Shiozaki, K. & Russell, P. Conjugation, meiosis, and the osmotic stress response are regulated by Spcl kinase through Atf1 transcription factor in fission yeast. *Genes Dev.* **10**, 2276–2288. <https://doi.org/10.1101/gad.10.18.2276> (1996).
40. Lawrence, C. L. *et al.* Regulation of *Schizosaccharomyces pombe* Atf1 protein levels by Sty1-mediated phosphorylation and heterodimerization with Pcr1. *J. Biol. Chem.* **282**, 5160–5170. <https://doi.org/10.1074/jbc.M608526200> (2007).
41. Bozonet, S. M. *et al.* Oxidation of a eukaryotic 2-Cys peroxiredoxin is a molecular switch controlling the transcriptional response to increasing levels of hydrogen peroxide. *J. Biol. Chem.* **280**, 23319–23327. <https://doi.org/10.1074/jbc.M502757200> (2005).
42. Stegmeier, F. & Amon, A. Closing mitosis: The functions of the Cdc14 phosphatase and its regulation. *Annu. Rev. Genet.* **38**, 203–232. <https://doi.org/10.1146/annurev.genet.38.072902.093051> (2004).
43. Queralt, E. & Uhlmann, F. Cdk-counteracting phosphatases unlock mitotic exit. *Curr. Opin. Cell Biol.* **20**, 661–668. <https://doi.org/10.1016/j.ceb.2008.09.003> (2008).
44. Mocciano, A. & Schiebel, E. Cdc14: A highly conserved family of phosphatases with non-conserved functions?. *J. Cell Sci.* **123**, 2867–2876. <https://doi.org/10.1242/jcs.074815> (2010).
45. Bassermann, F. *et al.* The Cdc14B-Cdh1-Plk1 Axis controls the G₂ DNA-damage-response checkpoint. *Cell* **134**, 256–267. <https://doi.org/10.1016/j.cell.2008.05.043> (2008).
46. Rodríguez-Gabriel, M. A., Watt, S., Bähler, J. & Russell, P. Upf1, an RNA helicase required for nonsense-mediated mRNA Decay, modulates the transcriptional response to oxidative stress in fission yeast. *Mol. Cell Biol.* **26**, 6347–6356. <https://doi.org/10.1128/MCB.00286-06> (2006).
47. Rodríguez-Gabriel, M. A. *et al.* RNA-binding protein Csx1 mediates global control of gene expression in response to oxidative stress. *EMBO J.* **22**, 6256–6266. <https://doi.org/10.1093/emboj/cdg597> (2003).
48. Day, A. M. & Veal, E. A. Hydrogen peroxide-sensitive cysteines in the Sty1 MAPK regulate the transcriptional response to oxidative stress. *J. Biol. Chem.* **285**, 7505–7516. <https://doi.org/10.1074/jbc.M109.040840> (2010).
49. Chen, J. S. *et al.* Comprehensive proteomics analysis reveals new substrates and regulators of the fission yeast Clp1/Cdc14 phosphatase. *Mol. Cell Proteomics* **12**, 1074–1086. <https://doi.org/10.1074/mcp.M112.025924> (2013).
50. Papadopoulou, K. *et al.* Regulation of cell cycle-specific gene expression in fission yeast by the Cdc14p-like phosphatase Clp1p. *J. Cell Sci.* **123**, 4374–4381. <https://doi.org/10.1242/jcs.073056> (2010).
51. Villarroja-Beltri, C. *et al.* Mammalian CDC14 phosphatases control exit from stemness in pluripotent cells. *EMBO J.* **42**, 111251. <https://doi.org/10.15252/emj.2022111251> (2022).
52. Guillaumot, M. *et al.* Cdc14b regulates mammalian RNA polymerase II and represses cell cycle transcription. *Sci. Rep.* **1**, 189. <https://doi.org/10.1038/srep00189> (2011).
53. Moreno, S., Klar, A. & Nurse, P. Molecular genetic analysis of fission yeast *Schizosaccharomyces pombe*. *Methods Enzymol.* **194**, 795–823. [https://doi.org/10.1016/0076-6879\(91\)94059-1](https://doi.org/10.1016/0076-6879(91)94059-1) (1991).

Acknowledgements

We thank members of 08 laboratory at the Centro de Investigación del Cáncer and R. Aligué (Universitat de Barcelona) for helpful discussions. We are particularly grateful to P. Russell (The Scripps Research Institute, CA, U.S), S. Grewal (Center for Cancer Research, U.S. National Institutes of Health), N. Jones (Paterson Institute for Cancer Research, Manchester, U.K.), R. Aligué (Universitat de Barcelona), Dr. Shiozaki (Nara Institute of Science and Technology) and K. Gould (Vanderbilt University, U.S) for fission yeast strains. AB and MS received financial support for this research work through Programa General de Conocimiento (BFU2015-69709-P and PID2019-109616GB-100) and Junta de Castilla y León (SA042P17 and SA103P20) grants from the Spanish Science, Innovation and Universities Ministry and Junta de Castilla y León. JAC was supported by a predoctoral fellowship from the Junta de Castilla y León. AB and MS Institution is supported by the “Programa de Apoyo a Planes Estratégicos de Investigación de Excelencia” cofunded by the Junta de Castilla y León and the European Regional Development Fund (CLC-2017-01).

Author contributions

J.A.C., S.A., S.M., J.Z. and S.R. generated strains, performed tenfold serial dilution assays and Northern and Western analyses, and characterized the localization of Flp1 under oxidative stress conditions. H.D-C. generated the Flp1-9A-GFP strain. M.P.S. performed quantitative real-time PCR, survival assays, coimmunoprecipitation and phosphatases assays. M.P.S. and A.B. designed the project, analyzed the data and wrote the manuscript.

Competing interests

The authors declare no competing interests.

Additional information

Supplementary Information The online version contains supplementary material available at <https://doi.org/10.1038/s41598-023-41869-w>.

Correspondence and requests for materials should be addressed to A.B. or M.P.S.

Reprints and permissions information is available at www.nature.com/reprints.

Publisher’s note Springer Nature remains neutral with regard to jurisdictional claims in published maps and institutional affiliations.



Open Access This article is licensed under a Creative Commons Attribution 4.0 International License, which permits use, sharing, adaptation, distribution and reproduction in any medium or format, as long as you give appropriate credit to the original author(s) and the source, provide a link to the Creative Commons licence, and indicate if changes were made. The images or other third party material in this article are included in the article’s Creative Commons licence, unless indicated otherwise in a credit line to the material. If material is not included in the article’s Creative Commons licence and your intended use is not permitted by statutory regulation or exceeds the permitted use, you will need to obtain permission directly from the copyright holder. To view a copy of this licence, visit <http://creativecommons.org/licenses/by/4.0/>.

© The Author(s) 2023